ACTA MECHANICA SINICA, Vol.8, No.2, May 1992 ISSN 0567-7718
Science Press, Beijing, China
Allerton Press, INC., New York, U.S.A.

THE INTERFACIAL CRACK BETWEEN TWO DISSIMILAR ELASTIC-PLASTIC MATERIALS*

Xia Lin (夏 霖) Wang Tzuchiang (王自强)

(*LNM, Institute of Mechanics, Chinese Academy of Sciences, Beijing* 100080, *China*)

ABSTRACT: This paper presents an exact asymptotic analysis on the interfacial crack between two dissimilar elastic-plastic materials. These two materials have identical hardening exponent ($n_1=n_2$) but different hardening coefficient ($\alpha_1\neq\alpha_2$). Two groups of the near-crack-tip fields have been obtained, which not only satisfy the continuity of both tractions (σ_θ, $\tau_{r\theta}$) and displacements (u_r, u_θ) on the interface, but also meet the traction free conditions on the crack faces. The first group of fields have the mode mixity M^P quite close to $M^P=1$ (MODE I) within the whole range $0\leqslant\alpha_1/\alpha_2<\infty$. As for the second group of fields, which is only obtained within the narrow range $0.9\leqslant\alpha_1/\alpha_2\leqslant 1$, it is found that the mode mixity changes sharply with the ratio value α_1/α_2.

KEY WORDS: asymptotic analysis, interfacial crack, mode mixity

I. INTRODUCTION

In recent years, the interface crack mechanics received much attentions, largely due to the common existance of interfacial fracture in lots of advanced materials such as polycrystalline intermetallic alloys, composites, and structural ceramics. The early research work on this field can be found in Williams[1], England[2], Erdogan[3], Rice and Sih[4] and so on. They have been clarified and extended by Hutchinson et al.[5], Rice[6] and Shih and Asaro[7] recently. In order to overcome the oscillation of singular stress and the interpenetration of crack faces existing in the classical solutions, some modified models of interface crack (such as Comninou[8], Achenbach et al.[9], Atkinson[10], Delale and Erdogan[11]) have been further developed. As for the interface cracks of the elastic-plastic materials, a significant progress was made by Shih and Asaro[7,12] in 1988. Through the detail full-field computational investigations by the finite element method, they found that the near tip fields of crack on bimaterial interfaces have the nearly separable form solutions of the HRR type in an annular region within the plastic zone. The other associated analyses include those of Zywicz and Parks[13], Guo and Keer[14], Gao and Lou[15] and Drugan[16].

Wang[17] presented an exact asymptotic analysis for a crack lying on the interface of an elastic-plastic material and linear elastic material. A separable singular stress field of the HRR type has been found in the plastic angular zone around crack tip.

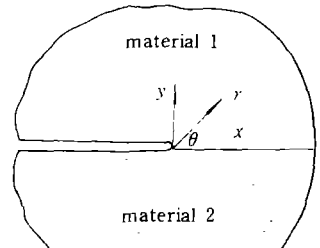

Fig.1 An interfacial crack

In this paper, an interfacial crack between two dissimilar power law hardening materials is analysed. Here, the hardening exponents are identical but the hardening coefficients are different for both materials. Two groups of asymptotic fields of the HRR type are obtained, which meet the continuity of both the tractions (σ_θ, $\tau_{r\theta}$) and the displacements (u_r, u_θ) on the interface ahead the crack tip. The crack faces open freely. Our results also indicate that, in one group of solutions the mode mixity only deviates a little from $M^P=1$, i.e. MODE I dominates, no matter what value the ratio α_1/α_2 takes. But in another group of solutions, which has been obtained within the region of $0.9\leqslant\alpha_1/\alpha_2\leqslant 1$, the mode mixity

Received 29 July 1991.
* The project supported by National Natural Science Foundation of China

changes rapidly just as the ratio value α_1/α_2 decreases from $\alpha_1/\alpha_2=1$.

II. BASIC EQUATIONS

Fig.1 shows an interfacial crack between material 1 and material 2. Under the uniaxial tension, both materials obey the Ramberg-Osgood formula:

$$\frac{\varepsilon}{\varepsilon_0}=\frac{\sigma}{\sigma_0}+\alpha\left(\frac{\sigma}{\sigma_0}\right)^n \tag{2.1}$$

where σ_0 and ε_0 are the yield stress and yield strain respectively. Between them there is a relation: $\varepsilon_0=\sigma_0/E$. α is the hardening coefficient and n is the hardening exponent. E is the Young's Modulus.

From Eq. (2.1) and the plasticity deformation theory, we can get the general constitutive relation as

$$\varepsilon_{ij}=\frac{(1+\nu)}{E}S_{ij}+\frac{(1-2\nu)}{3E}\sigma_{kk}\delta_{ij}+\frac{3}{2}\alpha\left(\frac{\sigma_e}{\sigma_0}\right)^{n-1}\frac{S_{ij}}{E} \tag{2.2}$$

where S_{ij} is the deviatoric stress component and σ_e is the effective stress. ν is the Poisson's ratio.

Throughout this paper, italic letters i, j, k are used for subscript indices running over value 1, 2, 3, and greek letters β, γ, ρ are used for subscript indices running over 1, 2.

Here, we assume that both materials have the same hardening exponent (i.e. $n_1=n_2$) but the different hardening coefficient (i.e. $\alpha_1\neq\alpha_2$). For the sake of simplicity, we further assume that two materials have the same yield stress, elastic modulus and Poisson's ratio, i.e. $\sigma_{o1}=\sigma_{o2}$, $E_1=E_2$, $\nu_1=\nu_2$. Afterwards, we will simply designate them as σ_0, E, ν and n.

For the plane strain, the stress-strain relation can be written in a brief form:

$$\varepsilon_{\beta\gamma}=\frac{(1+\nu)}{E}\sigma_{\beta\gamma}+\delta_{\beta\gamma}\frac{\Gamma}{E}\sigma_{\rho\rho}+\frac{\Lambda}{E}P_{\beta\gamma} \tag{2.3}$$

where $\sigma_{\rho\rho}=\sigma_r+\sigma_\theta$, $P_{\beta\gamma}=\sigma_{\beta\gamma}-\frac{1}{2}\sigma_{\rho\rho}\delta_{\beta\gamma}$, and

$$\Lambda=\frac{3}{2}\alpha\left(\frac{\sigma_e}{\sigma_0}\right)^{n-1}\qquad \Gamma=-(1+\nu)\nu+\left(\frac{1}{2}-\nu\right)^2\frac{\alpha(\sigma_e/\sigma_0)^{n-1}}{\alpha(\sigma_e/\sigma_0)^{n-1}+1} \tag{2.4}$$

If the stress function φ is introduced, stress components can be written as

$$\sigma_r=\frac{1}{r}\left(\frac{\partial\varphi}{\partial r}+\frac{1}{r}\frac{\partial^2\varphi}{\partial\theta^2}\right)\qquad \sigma_\theta=\frac{\partial^2\varphi}{\partial r^2}\qquad \tau_{r\theta}=-\frac{\partial}{\partial r}\left(\frac{1}{r}\frac{\partial\varphi}{\partial\theta}\right) \tag{2.5}$$

The relation between strain components and displacements are

$$\varepsilon_r=\frac{\partial u_r}{\partial r}\qquad \varepsilon_\theta=\frac{1}{r}\frac{\partial u_\theta}{\partial\theta}+\frac{u_r}{r}\qquad \varepsilon_{r\theta}=\frac{1}{2}\left(\frac{1}{r}\frac{\partial u_r}{\partial\theta}+\frac{\partial u_\theta}{\partial r}-\frac{u_\theta}{r}\right) \tag{2.6}$$

Let

$$\varphi=Kr^{s+2}\tilde{\varphi}(\theta) \tag{2.7}$$

where $s<0$.

Substituting Eq. (2.7) into (2.5), we obtain

$$\sigma_{\beta\gamma}=Kr^s\tilde{\sigma}_{\beta\gamma} \tag{2.8}$$

where

$$\tilde{\sigma}_r=\tilde{\varphi}''+(2+s)\tilde{\varphi}\qquad \tilde{\sigma}_\theta=(2+s)(1+s)\tilde{\varphi}\qquad \tilde{\tau}_{r\theta}=-(1+s)\tilde{\varphi}' \tag{2.9}$$

It is noted that $()'=d()/d\theta$.

In an asymptotic analysis for near-crack-tip field, the elastic strains and the second term are much small in comparison with the last term in Eq.(2.3), and therefore, can be neglected.

In this sense, we have

$$\varepsilon_{\beta\gamma}=\alpha_l \hat{K}^n r^{ns}\tilde{\varepsilon}_{\beta\gamma}(\theta) \tag{2.10}$$

where $l=1$ for $0\leqslant\theta\leqslant\pi$ and $l=2$ for $-\pi\leqslant\theta\leqslant 0$

$$\tilde{\varepsilon}_r=-\tilde{\varepsilon}_\theta=\frac{3}{4}\tilde{\sigma}_e^{n-1}(\tilde{\sigma}_r-\tilde{\sigma}_\theta) \qquad \tilde{\varepsilon}_{r\theta}=\frac{3}{2}\tilde{\sigma}_e^{n-1}\tilde{\tau}_{r\theta} \tag{2.11}$$

and $\hat{K}^n=(K/\sigma_o)^n\varepsilon_o$.

The effective stress is

$$\sigma_e=Kr^s\tilde{\sigma}_e(\theta) \tag{2.12}$$

where

$$\tilde{\sigma}_e=\left[\frac{3}{4}(\tilde{\sigma}_r-\tilde{\sigma}_\theta)^2+\tilde{\tau}_{r\theta}^2\right]^{1/2} \tag{2.13}$$

The strain compatibility equation is

$$\frac{1}{r}\frac{\partial^2}{\partial r^2}(r\varepsilon_\theta)+\frac{1}{r^2}\frac{\partial^2}{\partial\theta^2}\varepsilon_r-\frac{1}{r}\frac{\partial}{\partial r}\varepsilon_r-\frac{2}{r^2}\frac{\partial^2}{\partial r\partial\theta}(r\varepsilon_{r\theta})=0 \tag{2.14}$$

By using Eqs.(2.10), (2.11) and (2.9), the above equation can be represented as

$$\left[\frac{d^2}{d\theta^2}-ns(ns+2)\right][\tilde{\sigma}_e^{n-1}(\tilde{\varphi}''-s(s+2)\tilde{\varphi})]+4(1+ns)[\tilde{\sigma}_e^{n-1}(1+s)\tilde{\varphi}']'=0 \tag{2.15}$$

The traction free conditions on the crack faces require

$$\sigma_\theta|_{\theta=\pm\pi}=\tau_{r\theta}|_{\theta=\pm\pi}=0 \tag{2.16}$$

which lead to

$$\tilde{\varphi}(\pi)=\tilde{\varphi}'(\pi)=\tilde{\varphi}(-\pi)=\tilde{\varphi}'(-\pi)=0 \tag{2.17}$$

The displacements near the crack tip can be obtained by the integration of Eq.(2.6). Ignoring the rigid displacements, we get

$$u_\beta=\alpha_l \hat{K}^n r^{1+ns}\tilde{u}_\beta(\theta) \tag{2.18}$$

where $l=1$ for $0\leqslant\theta\leqslant\pi$ and $l=2$ for $-\pi\leqslant\theta\leqslant 0$, and

$$\tilde{u}_r=\tilde{\varepsilon}_r/(1+ns) \qquad \tilde{u}_\theta=(2\tilde{\varepsilon}_{r\theta}-\tilde{u}_r')/ns \tag{2.19}$$

On the interface, the continuity of tractions σ_θ, $\tau_{r\theta}$ and displacements require

$$\left.\begin{aligned}&[\sigma_\theta]=[\tau_{r\theta}]=0\\&[u_r]=[u_\theta]=0\end{aligned}\right\}\quad\theta=0 \tag{2.20}$$

or

$$\left.\begin{aligned}&\sigma_\theta^+-\sigma_\theta^-=0 \qquad \tau_{r\theta}^+-\tau_{r\theta}^-=0\\&u_r^+-u_r^-=0 \qquad u_\theta^+-u_\theta^-=0\end{aligned}\right\}\quad\theta=0 \tag{2.21}$$

Eq.(2.21) can be further represented as

$$\left.\begin{aligned}&R_1=\tilde{\varphi}^+(0)-\tilde{\varphi}^-(0)=0\\&R_2=\tilde{\varphi}'^+(0)-\tilde{\varphi}'^-(0)=0\\&R_3=\alpha_1\tilde{\varepsilon}_r^+(0)-\alpha_2\tilde{\varepsilon}_r^-(0)=0\\&R_4=\alpha_1[2(1+ns)\tilde{\varepsilon}_{r\theta}^+(0)-\tilde{\varepsilon}_r'^+(0)]-\alpha_2[2(1+ns)\tilde{\varepsilon}_{r\theta}^-(0)-\tilde{\varepsilon}_r'^-(0)]=0\end{aligned}\right\} \tag{2.22}$$

Eqs.(2.15), (2.17) and (2.22) comprise the governing equations for the asymptotic fields.

III. SOLUTION OF GOVERNING EQUATIONS

Homogeneous ordinary differential Eq.(2.15), together with homogeneous boundary conditions (2.17) and continuity conditions (2.22), define a nonlinear boundary value problem. Equivalently, it can be viewed as a nonlinear eigenvalue problem where the exponent of r in the solution for stresses is the eigenvalue. In order to solve this problem, let us assume that

$$\left.\begin{aligned} F_1(\theta)&=\tilde{\varphi}(\theta) & F_2(\theta)&=\tilde{\varphi}'(\theta)\\ F_3(\theta)&=\tilde{\varphi}''(\theta) & F_4(\theta)&=\tilde{\varphi}'''(\theta)\end{aligned}\right\} \tag{3.1}$$

Thus, Eq.(2.15) can be transformed into a set of one-order ordinary differential equations as follows.

$$\left.\begin{aligned} F_1'(\theta)&=F_2(\theta)\\ F_2'(\theta)&=F_3(\theta)\\ F_3'(\theta)&=F_4(\theta)\\ F_4'(\theta)&=RF\ (F_1,\ F_2,\ F_3,\ F_4)\end{aligned}\right\} \tag{3.2}$$

where

$$RF=\Omega/D_1$$

$$D_1=\frac{3}{4}\left[\tilde{\sigma}_e^{n-1}+\frac{3(n-1)}{4}\tilde{\sigma}_e^{n-3}(\tilde{\sigma}_r-\tilde{\sigma}_\theta)^2\right]$$

$$\Omega=2(ns+1)\tilde{\varepsilon}_{r\theta}'+ns(ns+2)\tilde{\varepsilon}_r-\frac{3}{4}\left[\left(\frac{(n-1)(n-3)}{4}\tilde{\sigma}_e^{n-5}((\tilde{\sigma}_e^2)')^2+\frac{(n-1)}{2}\tilde{\sigma}_e^{n-3}\tilde{\sigma}_{e3}\right)(\tilde{\sigma}_r-\tilde{\sigma}_\theta)+(n-1)\tilde{\sigma}_e^{n-3}(\tilde{\sigma}_e^2)'(\tilde{\sigma}_r'-\tilde{\sigma}_\theta')+\tilde{\sigma}_e^{n-1}((2+s)F_3-\tilde{\sigma}_\theta'')\right]$$

$$\tilde{\sigma}_{e3}=\frac{3}{2}(\tilde{\sigma}_r'-\tilde{\sigma}_\theta')^2+\frac{3}{2}(\tilde{\sigma}_r-\tilde{\sigma}_\theta)(\tilde{\sigma}_r''-(2+s)F_3)+6[(\tilde{\tau}_{r\theta}')^2+\tilde{\tau}_{r\theta}\tilde{\tau}_{r\theta}'']$$

Since the eigenfunction can only be determined to within a multiplicative constant, we can set $F_3(\pi)=1$ without loss of generality. Ultimately, the calculated stresses will be normalized so that $\{\tilde{\sigma}_e\}_{\max}=1$.

The shooting method is employed to solve the problem, and the corresponding integration of the system (3.2) is performed by the Runge-Kutta method with automatic step-size control.

Let

$$\left.\begin{aligned} F_3(\pi)&=1 & F_4(\pi)&=\eta_1\\ F_3(-\pi)&=\eta_2 & F_4(-\pi)&=\eta_3\\ s&=\eta_4\end{aligned}\right\} \tag{3.3}$$

where η_i $(i=1,\ 2,\ 3,\ 4)$ are unknown values, which will be determined as follows.

Using the initial conditions

$$F_1(\pi)=0 \qquad F_2(\pi)=0 \qquad F_3(\pi)=1 \qquad F_4(\pi)=\eta_1 \tag{3.4}$$

we can integrate Eq.(3.2) for θ from π to 0. In the same way, from the initial conditions

$$F_1(-\pi)=0 \qquad F_2(-\pi)=0 \qquad F_3(-\pi)=\eta_2 \qquad F_4(-\pi)=\eta_3 \tag{3.5}$$

we can also integrate Eq.(3.2) for θ from $-\pi$ to 0.

After the above integration, $F_i^+(0)$ and $F_i^-(0)$ $(i=1,\ 2,\ 3,\ 4)$ can be obtained. Through these values, Eq.(2.22) form a set of residual equations for 4 unknowns η_1, η_2, η_3 and η_4.

$$R_i(\eta_1,\ \eta_2,\ \eta_3,\ \eta_4)=0 \qquad (i=1,\ 2,\ 3,\ 4) \tag{3.6}$$

For solving the system (3.6), the Newton-Raphson method is utilized here:

$$J(\eta^k)\Delta\eta^k = -R(\eta^k) \tag{3.7}$$

and

$$\eta^{k+1} = \eta^k + \lambda\Delta\eta^k \tag{3.8}$$

where $\lambda \in (0, 1)$ is so chosen that the sum of squares of the residuals is reduced, i.e. the condition

$$\sum_{i=1}^{4} R_i^2(\eta^{k+1}) < \sum_{i=1}^{4} R_i^2(\eta^k) \tag{3.9}$$

is satisfied. The Jacobian matrix J is equal to $[\partial R_i/\partial\eta_j]$.

Our solving procedure is repeated until the condition of

$$\sum_{i=1}^{4} R_i^2(\eta^k) < 10^{-10}$$

is satisfied.

The preliminary computation indicated that the eigenvalue s is the same as that of the classical HRR solutions, i.e. $s = -\dfrac{1}{n+1}$.

IV. RESULTS AND DISCUSSIONS

In order to identify the relative strength of tensile and shear stresses ahead of the crack tip, Shih[8] defined a plastic mode mixity M^p by

$$M^p = \frac{2}{\pi}\tan^{-1}\left(\frac{\tilde{\sigma}_\theta(0)}{\tilde{\tau}_{r\theta}(0)}\right) \tag{4.1}$$

where M^p ranges from -1 to 1, with $M^p = 0$ for pure Mode II and $M^p = \pm 1$ for pure Mode I conditions in the near-field.

When $\alpha_1/\alpha_2 = 1$, it becomes a crack problem of the homogeneous material. In this case, our solutions do coincide with the two well-known solutions of the HRR field, which correspond to pure Mode I and pure Mode II crack respectively (shown as Fig.2 and Fig.3).

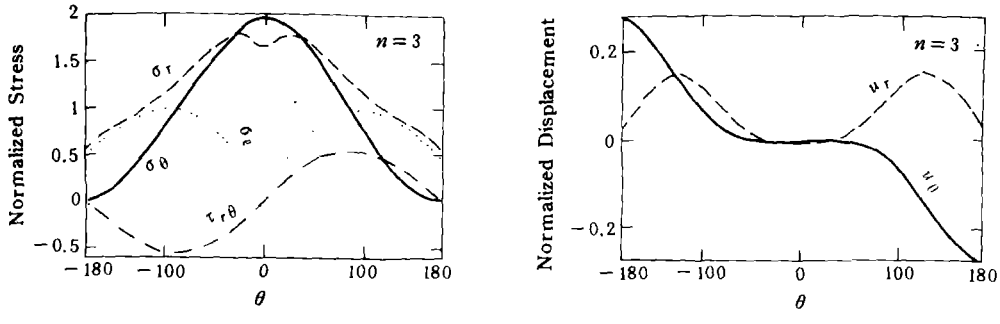

(a) Angular distribution of stresses (b) Angular distribution of displacement

Fig. 2 The near-crack-tip fields in homogeneous materials for $n=3$ (MODE I)
$\alpha_1=0.1$, $\alpha_2=0.1$ (MODE I)

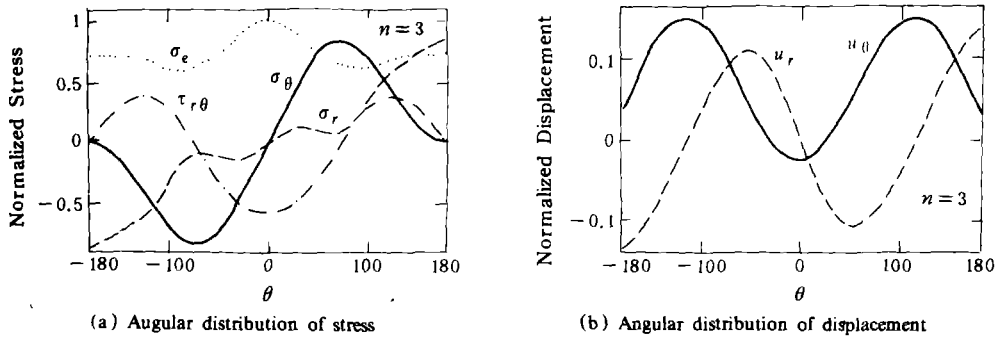

(a) Augular distribution of stress (b) Angular distribution of displacement

Fig. 3 The near-crack-tip fields in homogeneous materials for $n=3$ (MODE II)
$\alpha_1=0.1$, $\alpha_2=0.1$ (MODE II)

As the ratio between α_1 and α_2 deviates from $\alpha_1/\alpha_2=1$, we can imagine that there are also two solutions; among them, one has mode mixity M^p close to that of the pure MODE I (i.e. $M^p=\pm 1$); the other has mode mixity M^p close to that of the pure MODE II (i.e. $M^p=0$). Our results show that these two solutions certainly exist.

Within the region of $0\leqslant\alpha_1/\alpha_2\leqslant\infty$, we first found a group of solutions whose mode mixity M^p has little variation as the ratio value α_1/α_2 alters, and furthermore, they are always close to $M^p=\pm 1$. For example, as the ratio value α_1/α_2 changes from 1.0 to 0.0, the mode mixity of the near-tip field for $n=3$ increases from -1.0 to -0.960556 correspondingly and only alters a little (Fig.4, Fig.5). Alternatively, as the ratio α_2/α_1 changes from 1.0 to 0.0, M^p de-

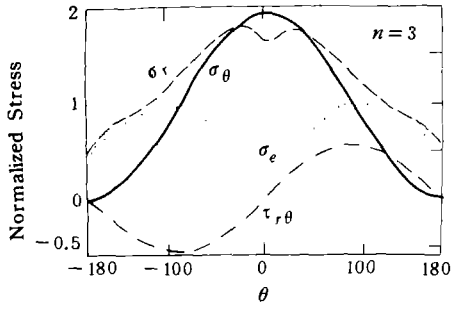

(a) Angular distribution of stresses
$\alpha_1=0.1$, $\alpha_2=0.2$ ($M^p=-0.989563$)

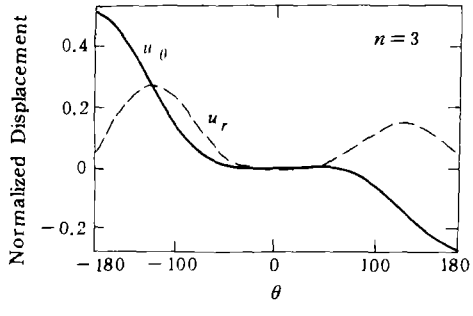

(b) Angular distribution of displacements
$\alpha_1=0.1$, $\alpha_2=0.2$ ($M^p=-0.989563$)

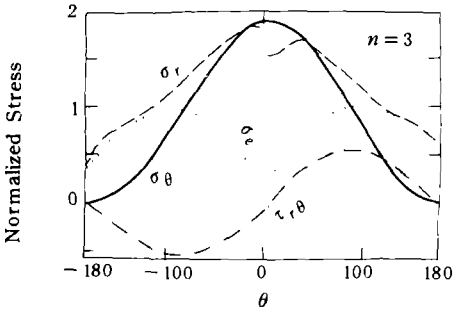

(c) Angular distribution of stresses
$\alpha_1=0.1$, $\alpha_2=1.0$ ($M^p=-0.970934$)

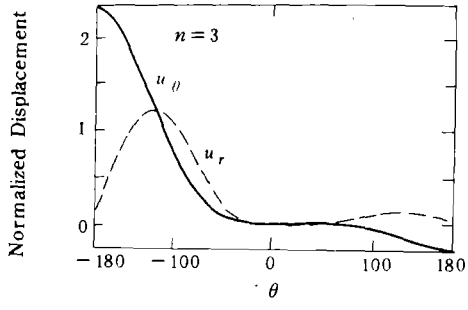

(d) Angular distribution of displacements
$\alpha_1=0.1$, $\alpha_2=1.0$ ($M^p=-0.970934$)

Fig.4 Interfacial crack-tip fields for $n=3$

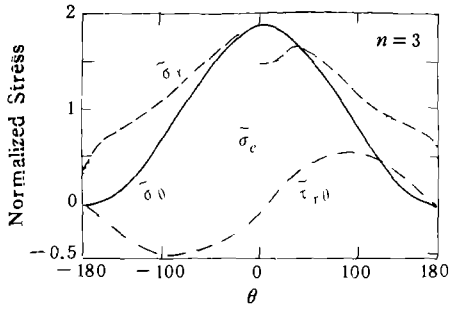

(a) Angular distribution of stresses
$\alpha_1=0.0$, $\alpha_2=0.1$ ($M^p=0.960556$)

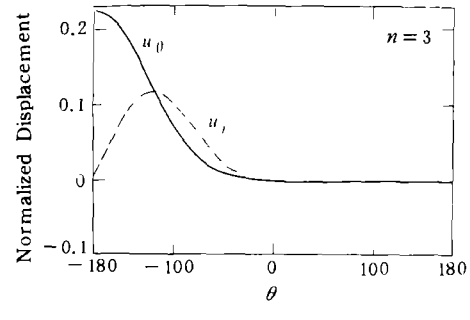

(b) Angular distribution of displacements
$\alpha_1=0.0$, $\alpha_2=0.1$ ($M^p=0.960556$)

Fig.5 Interfacial crack-tip fields for $n=3$

Table 1

α_1/α_2	M^p
0.0	−0.960556
0.1	−0.970934
0.2	−0.977615
1/3	−0.983909
0.5	−0.989563
1.0	−1.000000

Table 2

α_2/α_1	M^p
0.0	0.960556
0.1	0.970934
0.2	0.977615
1/3	0.983909
0.5	0.989563
1.0	1.000000

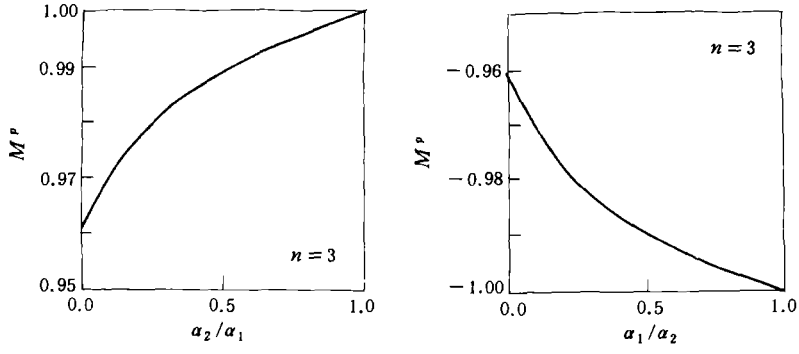

Fig.6 The mixed mode

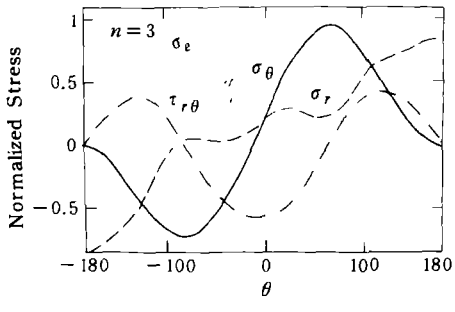

(a) Angular distribution of stresses
$\alpha_1=0.099$, $\alpha_2=0.1$ ($M^p=-0.246869$)

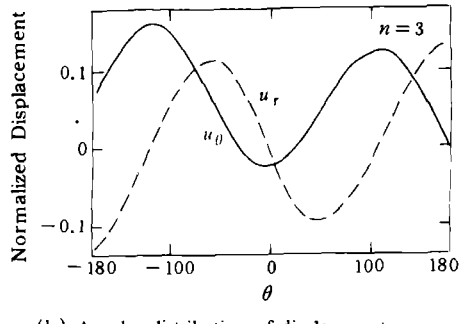

(b) Angular distribution of displacements
$\alpha_1=0.099$, $\alpha_2=0.1$ ($M^p=-0.246869$)

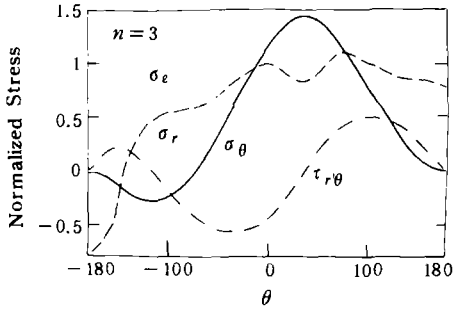

(c) Angular distribution of stresses
$\alpha_1=0.09$, $\alpha_2=0.1$ ($M^p=-0.773671$)

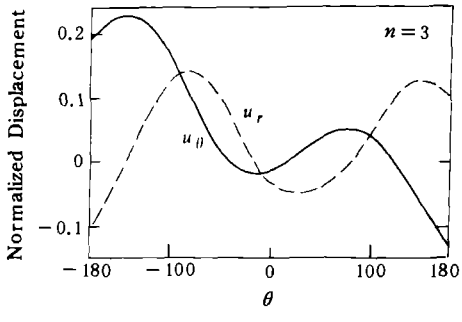

(d) Angular distribution of displacements
$\alpha_1=0.09$, $\alpha_2=0.1$ ($M^p=-0.773671$)

Fig.7 Interfacial crack-tip fields for $n=3$

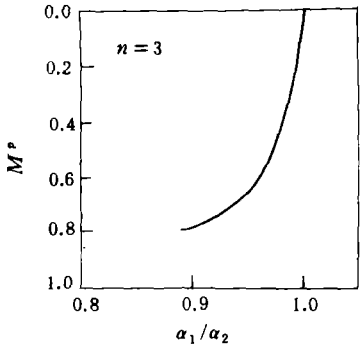

Fig.8 The mixed mode

Table 3

α_1/α_2	M^p
0.90	−0.773671
0.95	−0.656555
0.96	−0.607208
0.97	−0.535242
0.98	−0.423697
0.99	−0.246869
1.00	0.000000

$n=3$

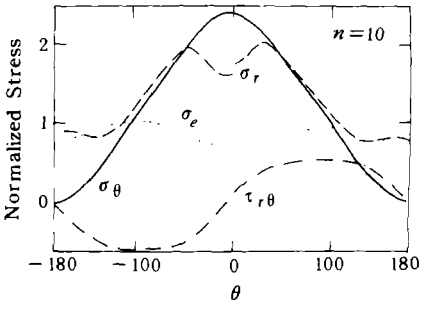

(a) Angular distribution of stresses
$\alpha_1=0.5$, $\alpha_2=0.1$ ($M^p=0.973222$)

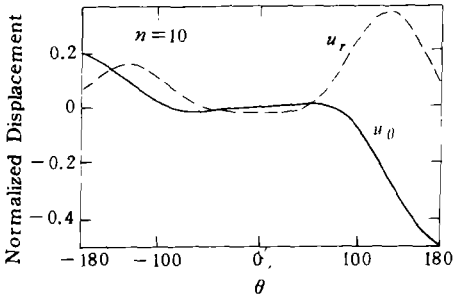

(b) Angular distribution of displacements
$\alpha_1=0.5$, $\alpha_2=0.1$ ($M^p=0.973222$)

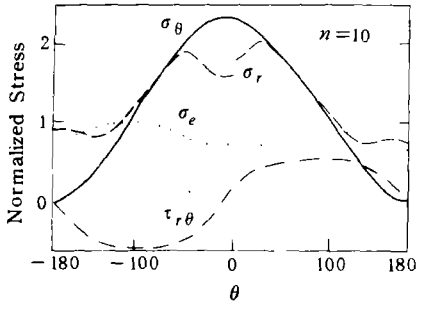

(c) Angular distribution of stresses
$\alpha_1=1.0$, $\alpha_2=0.1$ ($M^p=0.962147$)

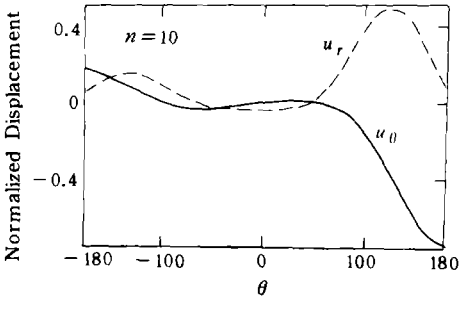

(d) Angular distribution of displacements
$\alpha_1=1.0$, $\alpha_2=0.1$ ($M^p=0.962147$)

Fig.9 Interfacial crack-tip fields for $n=10$

creases from 1.0 to 0.960556 correspondingly. The argument is the same as that of the above case. It is noted that when $\alpha_1=0$, the material system responds like that of a plastic deforming solid bonded to a rigid substrate in the asymptotic sense. The near-tip field in this case is shown in Fig.5. Its mode mixity M^p is equal to -0.969556. The variations of M^p with α_1/α_2 can be seen clearly in Fig.6, Table 1 and Table 2.

On the other hand, we searched for another group of fields (Fig.7) which have the mode mixity close to that of the MODE II (i.e. $M^p=0.0$). It is interesting to find that M^p changes very sharply when α_1/α_2 decreases slightly from $\alpha_1/\alpha_2\doteq 1.0$. Such sharp change of M^p with α_1/α_2 occurs within a narrow range $0.9\leqslant\alpha_1/\alpha_2\leqslant 1.0$, as shown in Fig.8 and Table 3.

Of course, within the above narrow range two solutions exist simultaneously for a given value of α_1/α_2. They correspond to two different M^p, respectively.

It is noted that above discussions are only associated with the near-tip fields for $n=3$.

When n is not equal to 3, our results also indicate that the near-tip fields have characteristics similar to those for $n=3$.

REFERENCES

1 Williams ML. Bull Seismol Soc America, 1959, 49: 199—204
2 England AH. J Appl Mech, 1965, 32: 400—402
3 Erdogan F.J Appl Mech, 1963, 30: 232—236
4 Rice JR and Sih GC. J Appl Mech, 1965, 32: 418—43
5 Hutchinson JW, Mear M and Rice JR. J Appl Mech, 1987, 54: 828—832
6 Rice JR. J Appl Mech, 1988, 55: 98—103
7 Shih CF and Asaro RJ. J Appl Mech, 1988, 55: 299—316
8 Comninou MJ. Appl Mech, 1977, 44: 631—636
9 Achenbach JD, Keer LM, Khetan RP and Chen SH. J Elasticity, (1979), 9: 397—424
10 Atkinson C.Int J Fract, 1977, 13: 807—820
11 Delale F and Erdogan F.J Appl Mech, 1988, 55: 317—324
12 Shih CF and Asaro RJ. J Appl Mech, 1989, 56: 763—779
13 Zywicz E and Parks DM. J. Appl Mech. 1989, 56: 577—584
14 Guo QX and Keer LM. J Mech Phys Solids, 1990, 38: 843—857
15 Gao YL and Lou ZW. Int J Fract, 1990, 43: 241—256
16 Drugan WJ. J Appl Mech, 1991, 58: 111—119
17 Wang TC. Engng Fract Mech, 1990, 37: 527—538